ADVANCED MATERIALS

stirring at room temperature. Following 120 min of stirring, this prehydrolyzed silica solution was mixed with a solution containing 1.78 g of the poly(ethylene oxide)–poly(propylene oxide)–poly(ethylene oxide) block copolymer ($EO_{20}PO_{70}EO_{20}$, Pluronic P123, BASF) dissolved in 30 mL of THF. The two solutions were mixed and stirred for a further 15 min. From this mixture, which had a final molar composition of TEOS/P123/H_2O/HCl/THF of 1:0.0094:5:0.0090:25, thin films were prepared by dip-coating onto cleaned quartz substrates at 75 mm min^{-1}. The films were stored at room temperature for 24 h and then extracted using ethanol, with a little concentrated HCl (37 %) being added under reflux conditions to remove the surfactant.

Preparation of Composite Films: The resultant films were extensively washed with ethanol and deionized water, and then dried at 150 °C for 24 h to remove the adsorbed water and dipped into 200 mL of dried toluene solution, which had been previously distilled over Zeolite 4A. After 30 min, 20 mL of TPED or APS were poured into the above toluene solution and refluxed for 12 h under a nitrogen atmosphere to obtain MTFs modified with NH_2 groups. The modified films were dipped into a 0.05 M $HAuCl_4$ aqueous solution for at least 2 h. $HAuCl_4$ could be effectively bonded due to the strong neutralization reaction with the basic NH_2 moieties [12]. The resultant films were calcined at 350 °C for 2 h under hydrogen atmosphere or air to obtain the gold-nanoparticle-loaded MTFs.

Received: July 7, 2004
Final version: December 2, 2004

[1] Y. Shi, C. Zhang, H. Zhang, J. H. Bechtel, L. R. Dalton, B. H. Robinson, W. H. Steier, *Science* **2000**, *288*, 119.
[2] Y. Hamanaka, A. Nakamura, S. Omi, N. D. Fatti, F. Vallee, C. Flytzanis, *Appl. Phys. Lett.* **1999**, *75*, 1712.
[3] K. Fukumi, A. Chayahara, K. Kadono, T. Sakaguchi, Y. Horino, M. Miya, J. Hayakawa, M. Satou, *Jpn. J. Appl. Phys., Part 2* **1991**, *30*, L742.
[4] H. B. Liao, R. F. Xiao, H. Wang, K. S. Wong, G. K. L. Wong, *Appl. Phys. Lett.* **1998**, *72*, 1817.
[5] S. T. Selvan, T. Hayakava, M. Nogami, Y. Kobayashi, L. M. Liz-Marzan, Y. Hamanaka, A. Nakamura, *J. Phys. Chem. B.* **2002**, *106*, 10 157.
[6] J. L. Shi, Z. L. Hua, L. X. Zhang, *J. Mater. Chem.* **2004**, *14*, 795.
[7] a) L. X. Zhang, J. L. Shi, J. Yu, Z. L. Hua, X. G. Zhao, M. L. Ruan, *Adv. Mater.* **2002**, *14*, 1510. b) C. Yang, H. Shen, K. Chao, *Adv. Funct. Mater.* **2002**, *12*, 143. c) V. Hornebecq, M. Antonietti, T. Cardinal, M. T. Delapierre, *Chem. Mater.* **2003**, *15*, 1993. d) H. Zhu, B. Lee, S. Dai, S. H. Overbury, *Langmuir* **2003**, *19*, 3974. e) Z. Konya, V. F. Puntes, I. Kiricsi, J. Zhu, J. W. Ager, M. K. Ko, H. Frei, P. Alivisatos, G. A. Somorjai, *Chem. Mater.* **2003**, *15*,1242.
[8] A. Fukuoka, H. Araki, Y. Sakamoto, N. Sugimoto, H. Tsukada, Y. Kumai, Y. Akimoto, M. Ichikawa, *Nano Lett.* **2002**, *2*, 793.
[9] a) Y. Yang, J. Shi, H. Chen, S. Dai, Y. Liu, *Chem. Phys. Lett.* **2003**, *370*, 1. b) L. Guo, G. Ma, Y. Liu, J. Mi, S. Qian, L. Qiu, *Appl. Phys. B.* **2002**, *74*, 253.
[10] a) J. L. Gu, J. L. Shi, L. M. Xiong, H. R. Chen, M. L. Ruan, *Micro. Meso. Mater.* **2004**, *74*, 199. b) S. Besson, T. Gacoin, C. Ricolleau, J. P. Boilot, *Chem. Commun.* **2003**, 360. c) Ö. Dag, O. Samarskaya, N. Coombs, G. A. Ozin, *J. Mater, Chem.* **2003**, *13*, 328. d) A. Fukuoka, H. Araki, J. Kimura, Y. Sakamoto, T. Higuchi, N. Sugimoto, S. Inagaki, M. Ichikawa, *J. Mater. Chem.* **2004**, *14*, 752.
[11] X. G. Zhao, J. L. Shi, B. Hu, L. X. Zhang, Z. L. Hua, *J. Mater. Chem.* **2003**, *13*, 399.
[12] S. Bharathi, O. Lev, *Chem. Commun.* **1997**, 2303.
[13] K. Esumi, J. Hara, N. Aihara, K. Usui, K. Torigoe, *J. Colloid Interface Sci.* **1998**, *208*, 578.
[14] a) J. L. Gu, J. L. Shi, H. R. Chen, L. M. Xiong, L. Li, M. L. Ruan, *Solid State Sci.* **2004**, *6*, 747. b) J. L. Gu, J. L. Shi, L. M. Xiong, H. R. Chen, W. Shen, M. L. Ruan, *Chem. Lett.* **2004**, *33*, 828.
[15] H. Inouye, K. Tanaka, I. Tanahashi, K. Hirao *Phys. Rev. B.* **1998**, *57*, 11 334.
[16] P. Zhou, G. J. You, Y. G. Li, T. Han, J. Li, S. Y. Wang, L. Y. Chen, Y. Liu, S. X. Qian, *Appl. Phys. Lett.* **2003**, *83*, 3876.
[17] Q. F. Zhang, W. M. Liu, Z. Q. Xue, J. L. Wu, S. F. Wang, D. L. Wang, Q. H. Gong, *Appl. Phys. Lett.* **2003**, *82*, 958.
[18] H. B. Liao, R. F. Xiao, J. S. Fu, P. Yu, G. K. L. Wong, P. Sheng, *Appl. Phys. Lett.* **1997**, *70*, 1.

Observation of High-Aspect-Ratio Nanostructures Using Capillary Lithography**

By *Kahp Y. Suh*,* *Se-Jin Choi*, *Seung J. Baek*, *Tae W. Kim*, and *Robert Langer*

The fabrication of periodic nanostructures is of great interest because of their potential applications in photonic crystals,[1–3] data storage,[4–6] and nanometer-scale biological sensors.[7,8] To enable such applications, unconventional methods that enable the fabrication of dense, large-area, periodic nanostructures with reasonable control over size and periodicity are required, since conventional photolithography and electron-beam lithography do not appear to be economically viable techniques.[9] Nano-imprint lithography and soft lithography are alternative, cost-effective, high-throughput lithographic techniques that could potentially replace photolithography for nanostructure fabrication in the sub-100 nm size régime.[10,11] In such parallel processes, various patterns are simultaneously formed by the physical contact of a hard or soft mold with a targeted substrate.

Recently, by simply combining essential features of nanoimprint and soft lithographies, we developed capillary lithography for patterning polymers over large areas.[12–15] This

[*] Prof. K. Y. Suh
School of Mechanical and Aerospace Engineering
Seoul National University
Seoul 151-742 (Korea)
E-mail: sky4u@snu.ac.kr
Dr. S.-J. Choi, Dr. S. J. Baek, T. W. Kim
Minuta Tech.
Center for Biotechnology Incubating
Shinlim-dong, Kwanak-gu, Seoul 151-742 (Korea)
Prof. R. Langer
Department of Chemical Engineering and
Division of Biological Engineering
Massachusetts Institute of Technology
Cambridge, MA 02139 (USA)

[**] This research was supported by a grant (04K1401-01710) from the Center for Nanoscale Mechatronics & Manufacturing, one of the 21st Century Frontier Research Programs, which are supported by Ministry of Science and Technology, Korea. This work was also supported in part by the Micro Thermal System Research Center of Seoul National University. K. Y. Suh thanks Dr. Sangyong Jon for providing the PEG copolymer and Dr. Hyunsik Yoon for providing the original master.

  DOI: 10.1002/adma.200401089

technique involves the direct placement of a patterned elastomeric mold onto a spin-coated polymer film on a substrate, followed either by formation of a negative replica of the mold by raising the temperature above the polymer's glass-transition temperature after solvent evaporation (temperature-induced capillarity),[12] or by direct molding prior to solvent evaporation (solvent-induced capillarity).[13] A potential concern with this technique is that a high-aspect-ratio poly(dimethylsiloxane) (PDMS) mold with sub-100 nm features is nearly impossible to obtain due to the low elastic modulus of PDMS (~1.8 MPa). Several researchers have reported that PDMS gives rise to deformation, buckling, or collapse of shallow relief features,[16,17] or that high surface tension causes rounding of sharp corners of imprinted patterns upon release from the PDMS master.[18] Indeed, this problem has also been an obstacle in most other soft-lithographic techniques for fabricating nanostructures.

To overcome these mechanical shortcomings of PDMS, a number of alternative molds have been reported, such as a composite PDMS,[19] bilayer PDMS,[20] photocurable PDMS,[21] a polyolefin mold,[22] PDMS with polymer-reinforced sidewalls,[23] a Teflon mold,[14,24] and a photocurable polyurethane acrylate mold.[25,26] Of these, the polyurethane acrylate mold turns out to be stiff enough for replicating dense, sub-100 nm features. In addition, this mold has a flexibility that allows large-area replication and a tunable elastic modulus, thus enabling its use in applications from imprinting to microcontact printing.

PDMS is presumably the rubbery polymer most permeable by air, and thus there have been no apparent problems concerning air permeation in pattern transfer.[27] We found, however, that the permeability issue came into play in the case of the polyurethane acrylate mold, especially when solvent-induced capillarity was utilized. For temperature-induced capillarity (i.e., after complete solvent evaporation), a small gap appeared to be present between the mold and the polymer (even when a pressure was applied to make conformal contact), facilitating air permeation through the gap. On the other hand, essentially no gap was present between the mold and the polymer in solvent-induced capillarity, since the solvent spontaneously wet the entire mold surface. One might expect that capillary rise into the void would not take place because of a capillarity-induced pressure buildup. Interestingly, we found that capillary rise still occurred, providing several unexpected nanostructures as a result of gas permeation and the different wetting conditions of the mold. In this communication, we report this interesting phenomenon along with various nanostructures formed by this method. In particular, we test a poly(ethylene glycol)-based (PEG-based), random copolymer, which has potential in biological applications.[28] We envision that high-density nanostructures of PEG polymers would provide a new route to fabricating novel biological sensors or constructing surfaces with unusual wetting properties. Also, we explore the possible mechanism of formation of the nanostructures, based on the interplay between hydrodynamic and Laplace pressures.

We used a polyurethane acrylate mold with dense nanopillar arrays, as shown in Figures 1a,b (heights ~ 300 nm, 500 nm, respectively). Depending on the etching conditions of the original silicon master, the height of the voids (i.e., the step height) of the mold could be controlled. To test the effects of the step height on pattern replication various heights ranging from ~ 300 nm to ~ 500 nm, were used throughout this work. The voids were of a truncated cone shape, with dimensions of 150–200 nm at the base and 70–100 nm at the top. The mold could be made positive or negative using self-replication, as reported previously.[26] During self-replication, trapped polymer radicals and remaining unsaturated acrylate in the first replica are removed by excessive exposure to UV light, usually for several hours. Then the same precursor is poured on top of the first replica, followed by UV exposure, thus obtaining the second replica. Figure 1c shows such a replicated negative mold from the positive molds in Figures 1a,b, which were used for generating protruding nanostructures. An example of the replicated sheet-type mold is shown in Figure 1d. For the polymer, we used a PEG-based, random copolymer that was reported previously,[28] or a water-soluble sulfonated polystyrene (SPS),[25] as described in the Experimental section. As long as water was used as the solvent and the concentration was low (< 10 wt.-%), we did not find any significant difference in the resulting nanostructures for both polymers.

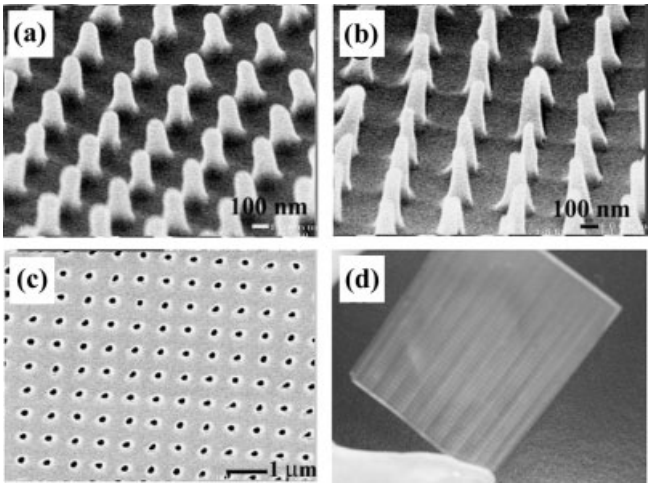

Figure 1. a,b) SEM images of the positive mold with step heights of 300 nm and 500 nm, respectively. c) SEM image of the replicated negative mold. d) An example of the sheet-type polyurethane acrylate mold.

To gain an understanding of the formation of the different nanostructures, we calculated a Laplace pressure for the polymer solution within the void of the mold, which gave

$$\Delta P_L = \frac{2\gamma}{r}\cos\theta \approx \frac{2\times 70\ \mathrm{mJ/m^2}}{75\ \mathrm{nm}}\cos\ 80^\circ = 3.2\ \mathrm{atm} \qquad (1)$$

where ΔP_L is the change in Laplace pressure, γ is the surface tension of the polymer solution, r is the radius of the nanopil-

ADVANCED MATERIALS

lar, and θ is the contact angle at the air/mold/solution interface (1 atm $\approx 101 \times 10^3$ Pa). The acrylate mold was hydrophobic in nature, yielding a contact angle of ~80°. This indicates that for an obtuse contact angle, capillary rise, rather than capillary depression, would take place. The initial air pressure within the void was assumed to be 1 atm, which would proportionally increase with increasing capillary rise. For example, the hydrodynamic pressure increased to 2 atm when the polymer solution rose to half the height of the mold voids, assuming no air permeation through the mold and solution. Thus, the maximum height, h_{max}, which is a function of the original step height of the mold, was calculated by equating the Laplace and increased hydrodynamic pressures. For the conditions used in the experiment, we obtained $h_{max} \approx (2/3)h$, where h is the initial step height of the mold. It is noted in this regard that the use of water as the solvent was essential for capillary rise within a *non-permeable* mold, in part due to the high surface tension of water (~72 mJ m^{-2}). To verify this, we tested using ethanol or methanol in place of water and the pattern replication turned out to be poor (data not shown). This could be attributed to the reduced Laplace pressure and the fast evaporation of the organic solvents.

We first investigated two types of PEG nanostructures with a step height of 300 nm, as shown in Figure 2. h_{max}, mentioned above, was estimated to be ~200 nm. To attain such a height, however, a number of conditions needed to be satisfied. First, conformal contact had to be maintained over the entire surface without many trapped bubbles. Otherwise, the air trapped in the voids in regions nearby could escape, leading to unexpected nanostructures with different heights. Second, the air-permeability of the mold needed to be very small, so that no air could escape through the mold. Third, the solubility of air in the polymer solution needed to be negligible, which is valid for the water that was used as solvent. Under these conditions, two types of nanostructures were observed in the experiment. The first is shown in Figure 2a. In this case, PEG nanopillars formed on the polymer surface with a diameter at the base (100–120 nm) that was reduced in comparison

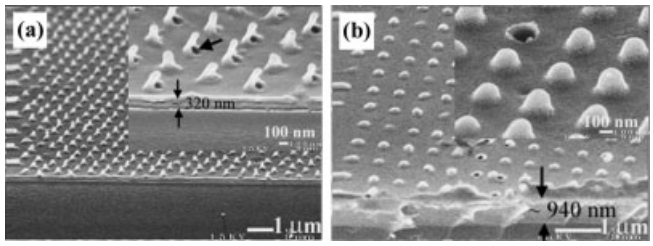

Figure 2. SEM images of the two types of nanostructures formed when the mold with a step height of 300 nm was used. a) Formation of nanopillars of reduced diameter. A dimple next to a nanopillar is indicated by an arrow in the inset. b) Formation of nano-hemispheres. Some hemispheres that were peeled off are shown as voids in the inset.

to that of the original mold (150–200 nm). A dimple was formed next to the nanopillars, an example of which is indicated by the arrow in the inset to Figure 2a. The height of the structure was measured to be about 300 nm, which is nearly the same as that of the step height of the mold.

We hypothesize that a difference in wetting dynamics at the walls of the voids could give rise to the formation of different nanostructures. As schematically illustrated in Figure 3, if wetting is initiated first at a certain position, the air pressure in the void is perturbed, such that the pressure at the wetted region could be higher than at the others. Accordingly, competition arises between the development of a uniformly curved meniscus and the continued rise in the wetting solution, while pushing air to the other dry regions. The formation of dimples next to the nanopillars is readily understood on the basis of this scenario. On the other hand, if a meniscus develops by overcoming the non-uniformity of the air pressure, the solution starts rising and stops at a height determined by the balance of the Laplace and hydrodynamic pressures, leading to a hemispherical structure as shown in Figure 2b. The structures were 170–200 nm in height, in satisfactory agreement with prediction. Some hemispheres were peeled off from the surface during the detachment of the mold, and are seen as voids in the figure.

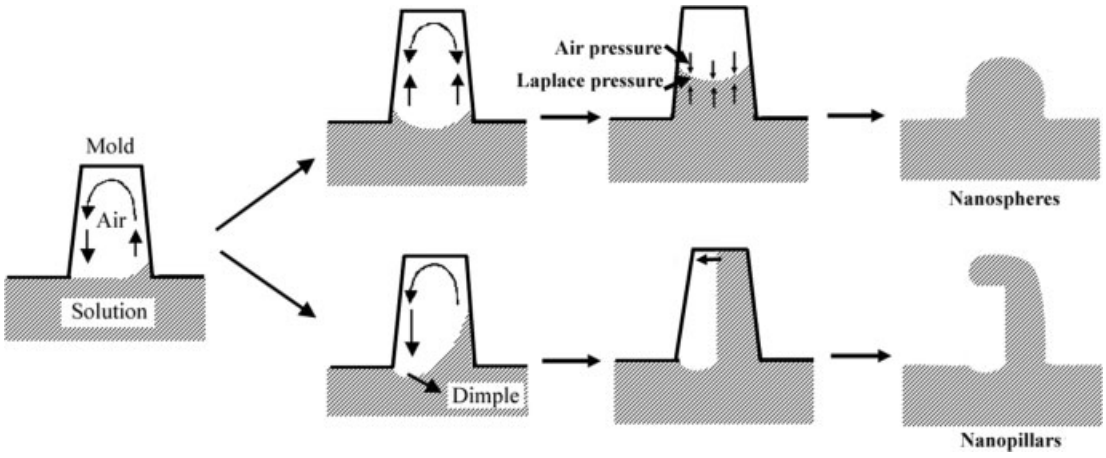

Figure 3. A schematic illustration for the formation of the two types of nanostructures, depending on the wetting conditions.

The criterion for determining the resultant structure could be related to the initial wetting conditions. Since the placement of the mold was performed manually, some defects or imperfections in the resulting structures were inevitably observed. Nonetheless, the first type of nanostructure (i.e., the nanopillars) was dominant on relatively thin films (< ~ 500 nm) whereas the second type (the nanospheres) was dominant on relatively thick films (> ~ 800 nm), suggesting that uniform contact with the aid of an abundant mass of water (i.e., uniform wetting) might lead to the second type (see the residual thicknesses in the figures). It is noted that the film thickness was measured after complete water evaporation, therefore its value does not reflect the initial film thickness.

We next investigated PEG nanostructures formed from molds with a 500 nm step height, and the results are shown in Figure 4. Similarly, nanopillars or nanospheres were observed depending on the film thickness. Interestingly, the shape was quite different for both nanostructures, in contrast to that for the mold with the 300 nm step height. As seen from Figures 4a,c, mushroom-like nanopillars of reduced diameter were observed, instead of the simple vertical pillars in Figure 2a. Dimples were formed next to the nanopillars (indicated by arrows in Fig. 2c), as mentioned earlier. This shape is quite striking, in that such a structure is not easily produced by other methods. The height of the nanopillars ranged from 450 to 500 nm, indicating that the voids of the mold were nearly completely filled with the PEG polymer.

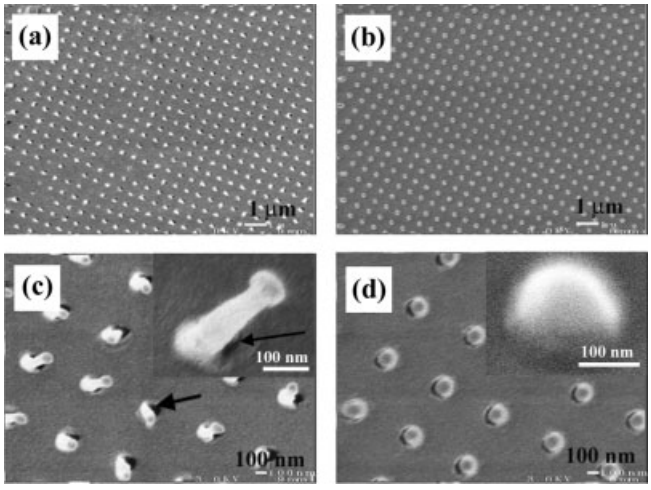

Figure 4. SEM images of the two types of nanostructures formed using the mold with a step height of 500 nm. a,c) Formation of mushroom-like nanopillars with a reduced diameter; large-scale (a) and magnified (c) views are shown. A dimple next to a nanopillar is indicated by an arrow in (c). b,d) Formation of nanospheres; large-scale (b) and magnified (d) views are shown.

The term "mushroom-like structure" used in this study, is meant to describe a structure in which the head is larger than the body. The difference between these structures and the vertical nanopillars is that, during their formation, the polymer solution wets the adjacent dry region in the mold void after reaching the ceiling, thus forming a head larger in size than the body (see the lower scheme in Fig. 3). The growth of the head continues until the Laplace pressure is in equilibrium with the air pressure in the void. In particular, the orientation of the mushroom's head and angle to the surface varied for each nanopillar because of the different wetting paths around the periphery of the nanopillar. Although mushroom-like structures were sporadically seen for molds with a 300 nm step height, as shown in Figure 2a, the possibility of mushroom formation was less likely than for the molds with the larger step heights. This was because the smaller step height lead to a faster increase of the air pressure. We foresee that mushroom-like structures could potentially be useful for optical and biological applications and for constructing surfaces with unusual wetting properties.

For the relatively thick film (i.e., with presumably more uniform wetting), regularly ordered nanospheres were generated on large areas, as shown in Figures 4b,d. The diameters (~ 150 to 170 nm) of the adjacent spheres and the sizes of the spaces between them (~ 500 nm) were in excellent agreement with those of the mold, suggesting that the nanospheres directly formed in the voids of the mold. Dewetting in the course of the molding process could be ruled out, since the substrate surface was not exposed and the film was relatively uniform. The formation of spheres could result from the contribution of the high surface tension of the PEG polymer (~ 42 mJ m^{-2})[29] and the increased hydrodynamic pressure within the voids.

Finally, we fabricated well-defined nanopillars with reduced diameters, as shown in Figure 5. While precise control over wetting conditions would be an obstacle for this purpose, we were able to create vertical nanopillars with a reduced diameter of ~ 90 nm for SPS (Fig. 5a) and ~ 110 nm for the PEG copolymer (Fig. 5b), using a mold with a step height of ~ 450 nm. The vertical nanopillars might not meet stringent pattern fidelity requirements since we frequently observed a mixture of vertical pillars, mushrooms, and spheres for the step heights tested. Nonetheless, the formation of vertical sidewalls was quite reproducible. The decrease in the diame-

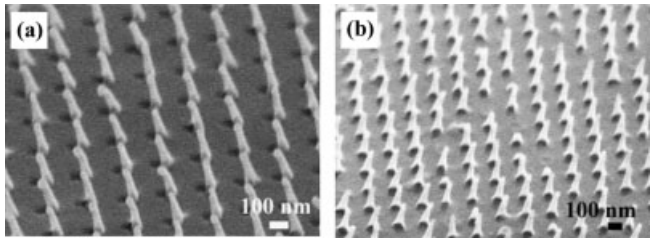

Figure 5. SEM images of well-defined, high-aspect-ratio nanopillars using a) SPS and b) the PEG copolymer. The diameters at the base are ~ 90 nm and ~ 110 nm, respectively.

ADVANCED MATERIALS

ter of the nanopillars was quite noticeable and would be useful in fabricating nanostructures with feature sizes smaller than those of the original master. The aspect ratio was as high as 5 for the nanostructures produced using SPS, and might be increased further with structures of smaller feature sizes. The black spots next to the pillars in the figures are dimples formed by pressure buildup.

In summary, we have presented the observation of several intriguing nanostructures, such as mushroom-like nanopillars, vertical nanopillars, and nanospheres, using capillary lithography with a UV-curable, polyurethane acrylate mold. It has been shown that air permeation during capillary rise plays an important role in pattern replication, which has not been previously observed in any type of nanofabrication involving PDMS molds. Depending on the film thickness of the polymer solution or the wetting conditions at the time of contact, nanopillars or nanospheres were observed for two different step heights of the mold used in the experiment. Furthermore, the step height could be adjusted to obtain well-defined vertical nanopillars with diameters less than that of the step height. This simple method would be potentially useful in fabricating unique nanostructures without resorting to other complicated, multistep methods.

Experimental

Fabrication of UV-Curable Mold: The UV-curable mold material consisted of a functionalized prepolymer with acrylate groups for crosslinking, a monomeric modulator, a photoinitiator, and a radiation-curable releasing agent for surface activity. Details on the synthesis and characterization of the polymer have been published elsewhere [26]. The UV-curable mold used in the experiment was a thin sheet with a thickness ranging from 0.3 to 1 mm (see Fig. 1d).

Polymers: We used a PEG-based random copolymer, poly(3-trimethoxysilyl)propyl methacrylate-*r*-polyethylene glycol methyl ether) (poly(TMSMA-*r*-PEGMA)) that has potential for use in biological applications. This polymer contains surface-reactive trimethoxysilyl groups as part of its backbone, which allows for the formation of multivalent bonds onto oxide surfaces, as well as multiple PEG chains. Detailed information on the synthesis and characterization of the polymer has been published elsewhere [28]. For comparison, we also used poly(sodium 4-styrenesulfonate) with a molecular weight of 200 000 (30 wt.-% in water, Aldrich). The polymer solution was diluted prior to use.

Capillary Lithography: A few drops of the polymer solution, of varying concentration (1–10 wt.-%), were placed on a silicon substrate and thin films were obtained by spin coating (Model CB 15, Headaway Research, Inc.) at 1000 rpm for 10 s. To make conformal contact, the polyurethane acrylate molds were carefully placed onto the surface and then the samples were stored overnight at room temperature to allow for evaporation of the solvent. The molds were peeled off using a sharp tweezer after complete evaporation of the solvent.

Scanning Electron Microscopy (SEM): Images were taken using a high-resolution scanning electron microscope (JEOL 6320FV) at an acceleration voltage of 15 eV and a working distance of 7 mm. Samples were coated with a 30 nm Au layer prior to analysis to prevent charging.

Contact-Angle Measurements: A Ramé–Hart goniometer (Mountain Lakes) equipped with a video camera was used to measure the static contact angles on drops ~3 μL in volume. Reported values represent averages of at least 3 independent measurements.

Received: July 9, 2004
Final version: October 15, 2004

[1] V. V. Poborchii, T. Tada, T. Kanayama, *Appl. Phys. Lett.* **1999**, *75*, 3276.
[2] S. M. Yang, G. A. Ozin, *Chem. Commun.* **2000**, 2507.
[3] M. C. Wanke, O. Lehmann, K. Muller, Q. Z. Wen, M. Stuke, *Science* **1997**, *275*, 1284.
[4] J. Y. Cheng, C. A. Ross, V. Z. H. Chan, E. L. Thomas, R. G. H. Lammertink, G. J. Vancso, *Adv. Mater.* **2001**, *13*, 1174.
[5] M. Hehn, K. Ounadjela, J. P. Bucher, F. Rousseaux, D. Decanini, B. Bartenlian, C. Chappert, *Science* **1996**, *272*, 1782.
[6] P. R. Krauss, S. Y. Chou, *Appl. Phys. Lett.* **1997**, *71*, 3174.
[7] A. J. Haes, R. P. Van Duyne, *J. Am. Chem. Soc.* **2002**, *124*, 10 596.
[8] K. B. Lee, S. J. Park, C. A. Mirkin, J. C. Smith, M. Mrksich, *Science* **2002**, *295*, 1702.
[9] Y. N. Xia, J. A. Rogers, K. E. Paul, G. M. Whitesides, *Chem. Rev.* **1999**, *99*, 1823.
[10] S. Y. Chou, P. R. Krauss, P. J. Renstrom, *Science* **1996**, *272*, 85.
[11] Y. N. Xia, G. M. Whitesides, *Annu. Rev. Mater. Sci.* **1998**, *28*, 153.
[12] K. Y. Suh, Y. S. Kim, H. H. Lee, *Adv. Mater.* **2001**, *13*, 1386.
[13] Y. S. Kim, K. Y. Suh, H. H. Lee, *Appl. Phys. Lett.* **2001**, *79*, 2285.
[14] D. Y. Khang, H. H. Lee, *Adv. Mater.* **2004**, *16*, 176.
[15] K. Y. Suh, H. H. Lee, *Adv. Funct. Mater.* **2002**, *12*, 405.
[16] E. Delamarche, H. Schmid, B. Michel, H. Biebuyck, *Adv. Mater.* **1997**, *9*, 741.
[17] A. Bietsch, B. Michel, *J. Appl. Phys.* **2000**, *88*, 4310.
[18] C. Y. Hui, A. Jagota, Y. Y. Lin, E. J. Kramer, *Langmuir* **2002**, *18*, 1394.
[19] H. Schmid, B. Michel, *Macromolecules* **2000**, *33*, 3042.
[20] T. W. Odom, J. C. Love, D. B. Wolfe, K. E. Paul, G. M. Whitesides, *Langmuir* **2002**, *18*, 5314.
[21] K. M. Choi, J. A. Rogers, *J. Am. Chem. Soc.* **2003**, *125*, 4060.
[22] G. Csucs, T. Kunzler, K. Feldman, F. Robin, N. D. Spencer, *Langmuir* **2003**, *19*, 6104.
[23] K. Y. Suh, R. Langer, J. Lahann, *Appl. Phys. Lett.* **2003**, *83*, 4250.
[24] D. Y. Khang, H. Kang, T. Kim, H. H. Lee, *Nano Lett.* **2004**, *4*, 633.
[25] Y. S. Kim, H. H. Lee, P. T. Hammond, *Nanotechnology* **2003**, *14*, 1140.
[26] S. J. Choi, P. J. Yoo, S. J. Baek, T. W. Kim, H. H. Lee, *J. Am. Chem. Soc.* **2004**, *126*, 7744.
[27] T. C. Merkel, V. I. Bondar, K. Nagai, B. D. Freeman, I. Pinnau, *J. Polym. Sci., Part B: Polym. Phys.* **2000**, *38*, 415.
[28] S. Y. Jon, J. H. Seong, A. Khademhosseini, T. N. T. Tran, P. E. Laibinis, R. Langer, *Langmuir* **2003**, *19*, 9989.
[29] J. Brandup, E. H. Immergut, *Polymer Handbook*, Wiley, New York **1989**.

Self-Assembled Silicon Nanotubes Grown from Silicon Monoxide

By *Yang-Wen Chen*, *Yuan-Hong Tang*,* *Li-Zhai Pei*, and *Chi Guo*

The successful synthesis of carbon nanotubes (CNTs)[1] and silicon nanowires (SiNWs)[2,3] has stimulated great interest in nanomaterials for their novel physical properties and potential applications in nanomaterials and optic electronics.[4]

[*] Prof. Y. H. Tang, Y. W. Chen, Dr. L. Z. Pei, C. Guo
College of Materials Science and Engineering
Hunan University
Changsha 410082 (P.R. China)
E-mail: yhtang@hnu.cn

  DOI: 10.1002/adma.200401381